

Document downloaded from:

<http://hdl.handle.net/10251/123502>

This paper must be cited as:

Galindo, J.; Climent, H.; Varnier, O.; Patil, CY. (2018). Effect of boosting system architecture and thermomechanical limits on diesel engine performance: Part II - Transient operation. *International Journal of Engine Research*. 19(8):873-885.  
<https://doi.org/10.1177/1468087417732264>



The final publication is available at

<http://doi.org/10.1177/1468087417732264>

Copyright SAGE Publications

Additional Information

# Effect of boosting system architecture and thermomechanical limits on diesel engine performance. Part-II: Transient Operation

Jose Galindo, Hector Climent, Olivier Varnier<sup>†</sup>, Chaitanaya Patil\*  
CMT-Motores Térmicos, Universitat Politècnica de València, Valencia 46022, Spain.,  
<sup>†</sup>Jaguar Land Rover Ltd., UK.,  
\*e-mail : chpa7@mot.upv.es

07/11/2016

## Abstract

Nowadays, internal combustion engines developments are focused on efficiency optimization and emission reduction. Increasing focus on world harmonized way to determine the performance and emissions on WLTP cycles is demanding to optimize the engines within transient operations. To achieve these, downsized or downspeeded engines are required which can reduce fuel consumption and  $CO_2$  emission. However, these technologies ask for efficient charging system. This paper consist of study of different boosting architectures (single stage and two stage) with combination of different charging system like super-chargers, e-boosters etc. A parametric study is been carried out with a 0D engine model to analyze and compare different architectures on same base engine. The impact of thermomechanical limits, turbo sizes and other engine development options characterizations are proposed to improve Fuel consumption, maximum power and performance of the downsized/downspeeded diesel engines during the transient operations.

## 1 Introduction

To characterize the new turbocharging architectures, a comprehensive study has been carried out with 0D engine model responding to specific objectives. The model consist of a phenomenological combustion model and a 0D filling and emptying model. In the first part of this paper we have covered analysis of an engine and the boosting system performance under steady state

24 operations. In this paper, the results obtained in single stage operations will be first reported to  
25 characterize the turbolag of small turbochargers. Then, the results obtained in two-stage oper-  
26 ations will be presented to determine the impacts of the main turbocharger on time responses  
27 and to analyze the transient behavior of eBooster and supercharger configurations.

## 28 **2 Methodology: Transient Operations**

29 The cold transient tests at 1000 rpm have been simulated with the different boosting architec-  
30 tures for three engine displacements. These transient cycles are critical for the charging systems  
31 due to low gas mass flows and thermal inertias. Time responses obtained under these transient  
32 operations are therefore quite representative of the performance of both engine and boosting  
33 architectures. In modern engines development, it is generally assumed that 'one second' repre-  
34 sents a good time response to reach the maximum low-end torque starting from low load, while  
35 'two seconds' corresponds to poor transient abilities. Between both times, transient responses  
36 can be judged acceptable or not according to the specific application. For the simulations, the  
37 pressure losses characteristics of Engine (from the 1st part of the paper) components have been  
38 employed on the 2.3l engine and then scaled on the 1.6l and 1.2l engines to obtain the same  
39 pressure drops under the corresponding gas mass flows. Compressor outlet and exhaust man-  
40 ifold temperatures have not been restrained in the calculations but specific control strategies  
41 have been implemented on the turbines actuators to avoid excessive exhaust manifold pressure  
42 (limitation fixed at 4.5 bar). The smoke limiter has been calibrated with a maximum fuel to  
43 air ratio ( $\lambda$ ) of 0.9 and advanced in cylinder pressure limitations have been retained in the  
44 cylinders.

	Type	Wheel diameter [mm]	Inertia [ $10^{-6}kg/m^2$ ]	Peak efficiency [%]
turbine A	VGT	35	4.32	65.5
turbine A_30	VGT	30	1.29	63
turbine A_25	VGT	25	0.43	60
turbine A_20	VGT	20	0.11	56
Turbine 1	FGT	35.5	3.59	65.5
Turbine 2	FGT	34	2.76	64.5
Turbine 3	FGT	31	1.58	63.5
Turbine 3_25	FGT	25	0.43	60
Turbine 3_20	FGT	20	0.11	56
Turbine 3_15	FGT	15	0.02	51

Figure 1: turbine characteristics

	Wheel diameter [mm]	Inertia [ $10^{-6}kg/m^2$ ]	Peak efficiency [%]
Compressor A	41	1.86	73.8
Compressor A_34	34	0.71	72.8
Compressor A_29	29	0.31	72.3

Figure 2: compressor characteristics

### 3 Turbocharger Response

As we know, turbolag phenomenon is influenced by three main factors which are the turbine swallowing capacity, both compressor and turbine efficiencies and turbocharger inertia. A sensitivity study has thus been carried out on these factors to quantify their influences on transient response. For the impact of swallowing capacities, the different turbines from figure 1 have been coupled to different compressors figure 2 and then connected to the 2.3l engine.

The transient results obtained in single stage operations are shown in figure 3. Even though

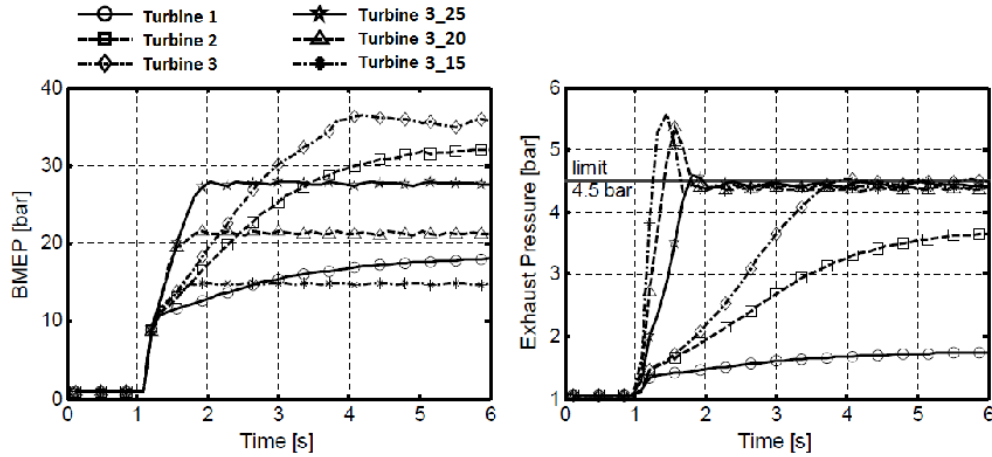


Figure 3: Influence of turbine swallowing capacity on transient performance during cold transient test cycles at 1000rpm on the 2.3l engine.

52 the turbine 1 is able to provide relatively high low-end torque in steady conditions, it can be  
 53 observed how its power ability is too small under low gas mass flow and cold conditions to  
 54 produce acceptable transient responses. Reducing the turbine effective section improves this  
 55 situation and here a low end-torque objective of 30 bar BMEP can be reached in 3 seconds and  
 56 2 seconds with the turbine 2 and 3 respectively. At 20 bar BMEP, the turbine 3 swallowing  
 57 capacity represents a good match for the 2.3l engine achieving the torque objective in around 1  
 58 second. This time response can further be enhanced to 0.6 second using the Turbine 3\_25 but  
 59 its small effective section leads rapidly to choked conditions restricting the maximum reachable  
 60 BMEP to 27 bar due to exhaust manifold pressure limitations. With the turbine almost choked,  
 61 reducing even more the swallowing capacity strongly decrease the maximum BMEP and does  
 62 not improve the time response. In fact at the beginning of the transient, the benefits of smaller  
 63 turbine section are offset by higher engine backpressures. For a given engine displacement,

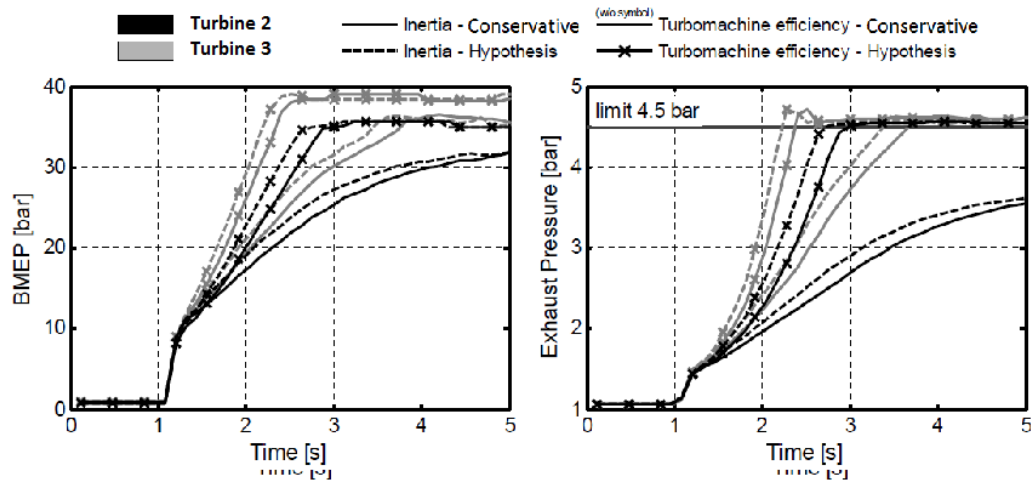


Figure 4: Influence of turbocharger efficiencies and inertia on transient performance during cold transient test cycles at 1000rpm on the 2.3l engine.

64 there is therefore a limit in turbine size reduction to maximize transient performance and here  
 65 for the 2.3l engine an objective of 30 bar BMEP cannot be achieved in 1 second with small  
 66 conservative turbine designs.

67 Regarding turbocharger efficiencies and inertias, variations of 10 points and 25% have been  
 68 considered respectively. The simulations have been performed with the Turbine 2 and 3 fitted in  
 69 the 2.3l engine. The results are shown in figure 4. As these turbines already have relatively low  
 70 inertias, it can be noticed that the use of advanced material to significantly reduce their inertia  
 71 has limited consequences on transient responses. Here, benefits of only 0.2-0.3 second have  
 72 been obtained with 25% inertia reduction. However, the improvements in turbocharger effi-  
 73 ciencies present important potential to enhance transient performance. In fact, increasing by 10  
 74 points the turbocharger efficiencies allow the time responses to be reduced by 50% and higher  
 75 BMEP to be reached. With these efficiencies variations, the objective of 30 bar BMEP can now  
 76 be achieved in 1 second using a turbine slightly smaller than the Turbine 3. Small effective

77 sections and efficient designs are therefore the fundamental combination to reduce turbo-lag  
78 phenomena. Analyzing the turbine requirements for the different engine displacements, it can  
79 be observed in figure 5 for an objective of 20 bar BMEP that the Turbine 3 provides a good tran-  
80 sient response on the 2.3l engine but its swallowing capacity is too large to have some power  
81 abilities on the 1.6l engine. The corresponding time response is thus extremely slow and a 20%  
82 smaller turbine (Turbine\_25) has to be developed to reach the torque objective within 1 second.  
83 On the 1.2l engine, the low gas mass flows are even more critical and a 35% smaller turbine  
84 (Turbine 3\_20) is required to reach the same performance. These scaling values can obviously  
85 be reduced if more efficient designs are developed in parallel to small swallowing capacities.  
86 For an objective of 30 bar BMEP.

87 efficiencies improvements are also essential and the trends underlined on the 2.3l engine can  
88 be generalized to the other engine displacements. So, turbines slightly smaller and significantly  
89 more efficient than the ones retained for the 20 bar BMEP objective need to be developed to  
90 reach this power level within 1 second. With VGT turbines, it can be noticed for the 2.3l  
91 engine that the smallest VGT available in the automotive market takes the same time to reach  
92 20 bar BMEP as the smallest FGT. In fact, the benefits of smaller swallowing capacity obtained  
93 in closed position are offset by lower efficiency and higher inertia. Applying to the VGT the  
94 scaling factors previously defined for the FGT, this effect can also be verified for the 1.6l and 1.2l  
95 engines where the turbine A\_30 and turbine A\_25 produce similar time responses as the Turbine  
96 3\_25 and Turbine 3\_20 respectively. At 20 bar BMEP, fitting a VGT in the HP stage presents  
97 thus little interest for the 2.3l engine but, for other engine displacements, the bigger wheel  
98 diameters involved can justify its use to reduce the efforts in small turbine designs development  
99 (wheel diameter differences of around 5mm). For higher BMEP, VGT are progressively open  
100 at the end of the transient to limit choked conditions adapting their swallowing capacity to the  
101 gas mass flows, so no power is lost through a wastegate. Transient performances are therefore

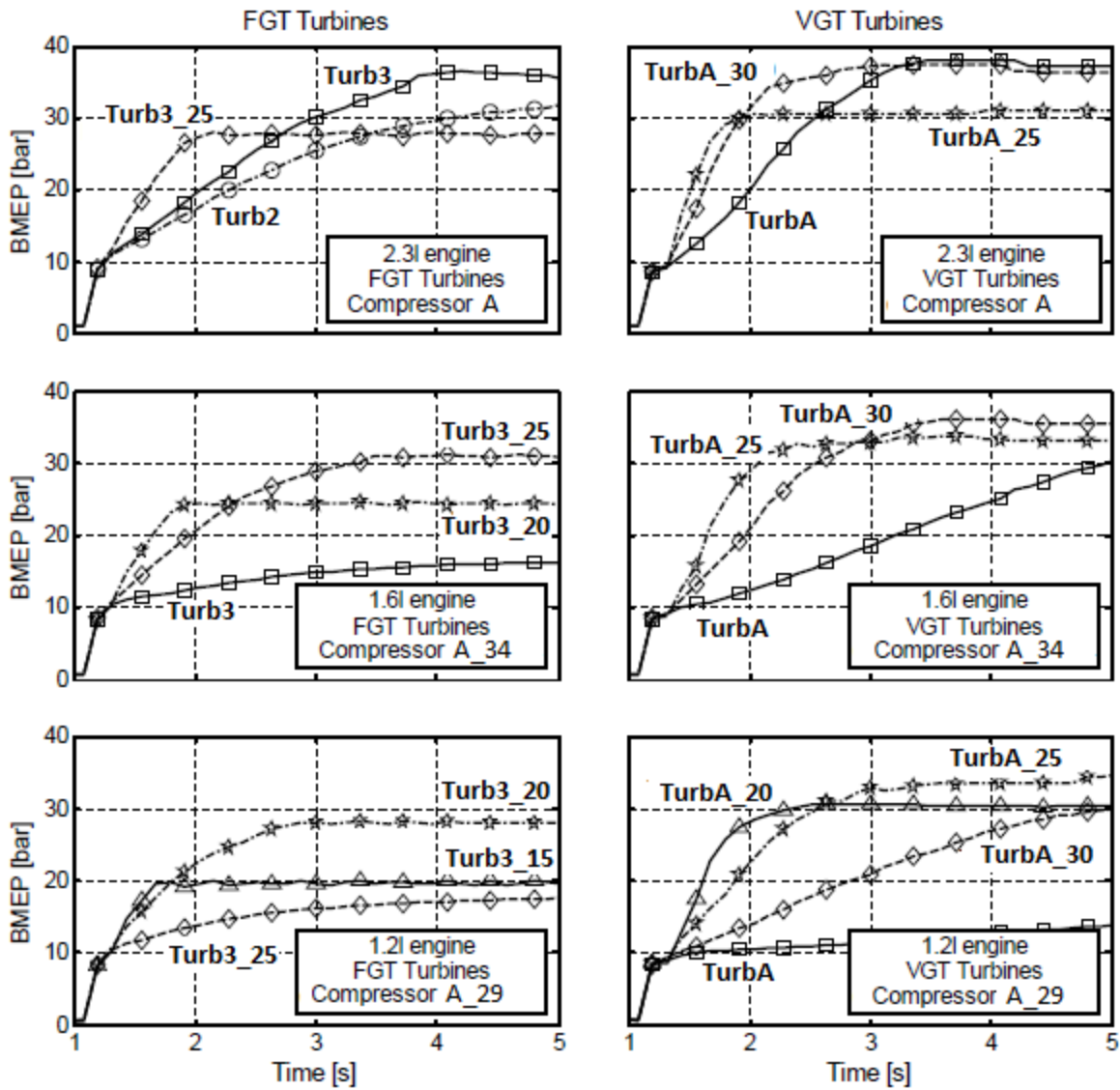


Figure 5: Turbine requirements to fulfill transient performance objectives in downsized-downspeeded engines during cold transient test cycles at 1000rpm. efficiencies



102 enhanced with VGT and efficiencies improvements are less critical than for FGT. In that way,  
103 the objective of 30 bar BMEP within 1 second can be achieved with conservative turbine designs  
104 (Turbine A\_30, turbine A\_25 and turbine A\_20 for the 2.3l, 1.6l and 1.2l engines respectively) or  
105 with the VGT defined at 20 bar BMEP increasing relatively their efficiencies. The use of VGT  
106 at this power level can thus reduce development efforts not only in small effective sections but  
107 also in highly efficient designs.

## 108 **4 Two-Stage Performance**

### 109 **4.1 Two Stage Turbocharging Architecture**

110 In a two-stage turbocharging architecture, the main turbocharger can also have some abilities to  
111 produce boost at low engine speeds depending on its minimum swallowing capacity and VGT  
112 actuator strategies. This boost production has an impact on the second turbocharger operating  
113 conditions and on the whole transient performance. To illustrate these effects, simulations have  
114 been realized on the 2.3l engine with a FGT turbine 3 in the HP stage (wastegate closed) and  
115 a e-booster in the LP stage. A relatively small turbocharger has especially been retained in the  
116 LP stage to increase boost abilities at low speeds and amplify the main turbocharger influences.  
117 The results are shown in figure 6 where the transient responses obtained in two stage operations  
118 varying VGT position are compared to the response previously obtained in single stage opera-  
119 tions with the same HP turbocharger. As it can be observed, the fastest transient is achieved in  
120 single stage operations when the small turbocharger works alone without any interactions from  
121 the LP stage. In two stage operations, even though 50% to 100% VGT open- ings produce here  
122 similar results, the time responses increase closing the VGT as more energy is recovered by the  
123 main turbocharger.

124 This behavior is explained in figure 7 with the different operating conditions plotted in the  
125 characteristics maps. Increasing the main turbocharger work increases the gas density in the

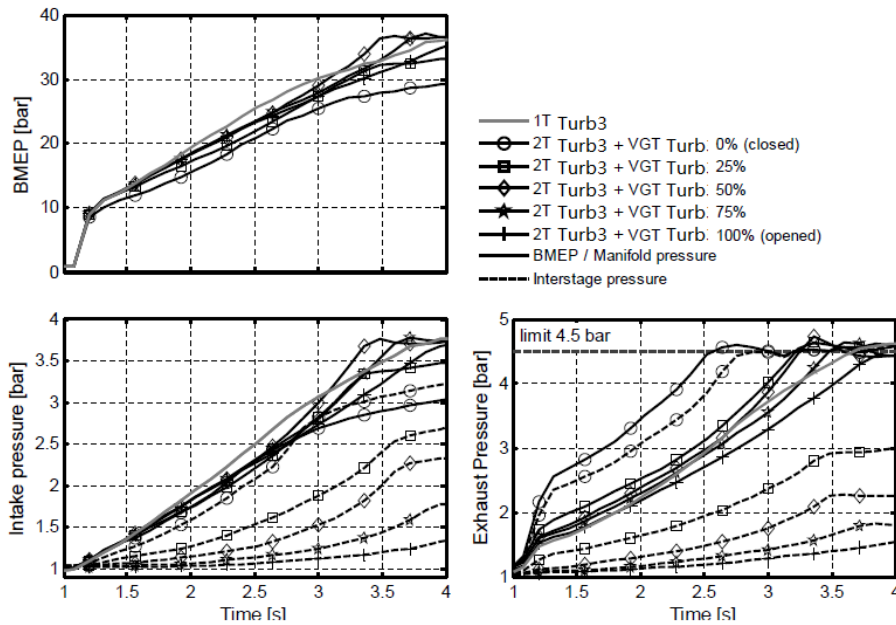


Figure 6: Effect of main turbocharger matching and VGT actuator strategies on transient performance (cold transient test cycles at 1000rpm on the 2.3l engine).

126 HP stage. The adapted gas mass flows are therefore reduced in the second turbine and, having  
 127 a given swallowing capacity, its power ability is lowered. This decrease of boost in the HP  
 128 stage is more or less offset by the main turbocharger but, as the LP stage has a higher inertia,  
 129 transient responses are deteriorated. So, the VGT has to be maintained in an open position  
 130 to optimize the transient responses in a two-stage turbocharging configuration equipped with a  
 131 VGT in the LP stage. Comparing the results obtained at 100% VGT opening with those obtained  
 132 in single stage operations, slight differences exist here between both time responses because  
 133 the main turbocharger has a relatively small matching and the VGT produced some work even  
 134 in full open position. With a bigger matching more adapted to this engine displacement, these  
 135 differences would be insignificant. So, the conclusions found in the previous section are also  
 136 valid in two-stage operations and the development of small high efficient turbines stay critical  
 137 to fulfill the performance requirements of future downsized-downspeeded engines.

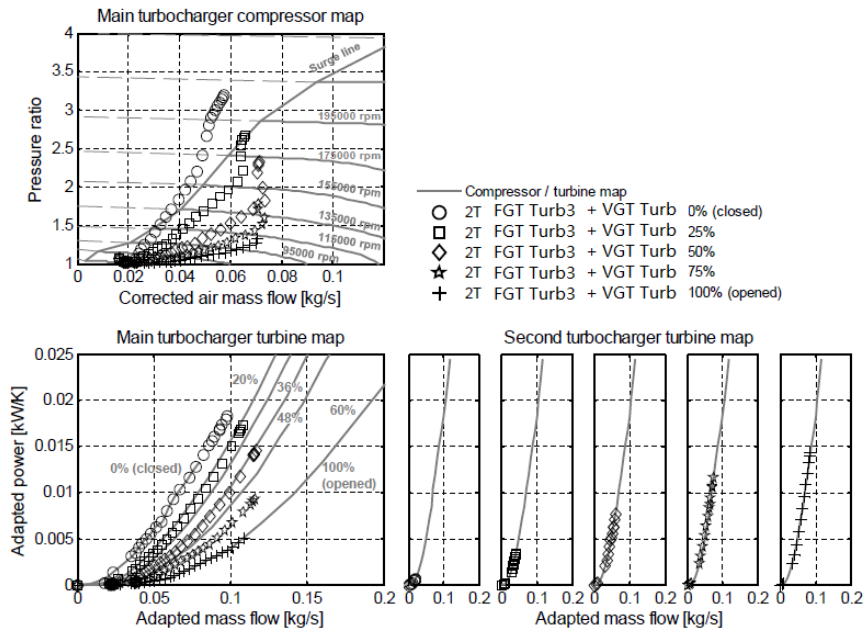


Figure 7: Interactions between HP and LP turbochargers during transient operations as a function of main turbocharger matching and VGT actuator strategies (cold transient test cycles at 1000rpm on the 2.3l engine).

## 4.2 Two-Stage E-booster Architecture

In a 2T eBooster configuration, transient responses depend on the electric power supplied by the vehicle network and on the turbocharger boost abilities. As there is no interaction between the HP and LP stages in the exhaust side, the VGT is maintained in a closed position to optimize the turbine work production. According to the turbocharger matching, this position can be the closest VGT opening to generate the maximum power with the smallest turbine swallowing capacity, or the VGT opening that maximizes boost pressure preventing compressor surge. To analyze the main characteristics of 2T eBooster architecture responses, calculations have been carried out on the 2.3l engine with a 4 kW eBooster. For the eBooster, the compressor inertia has been doubled to simulate representative eBooster accelerations considering also a rough motor inertia [150, 247]. The results obtained under full eBooster electric power are shown

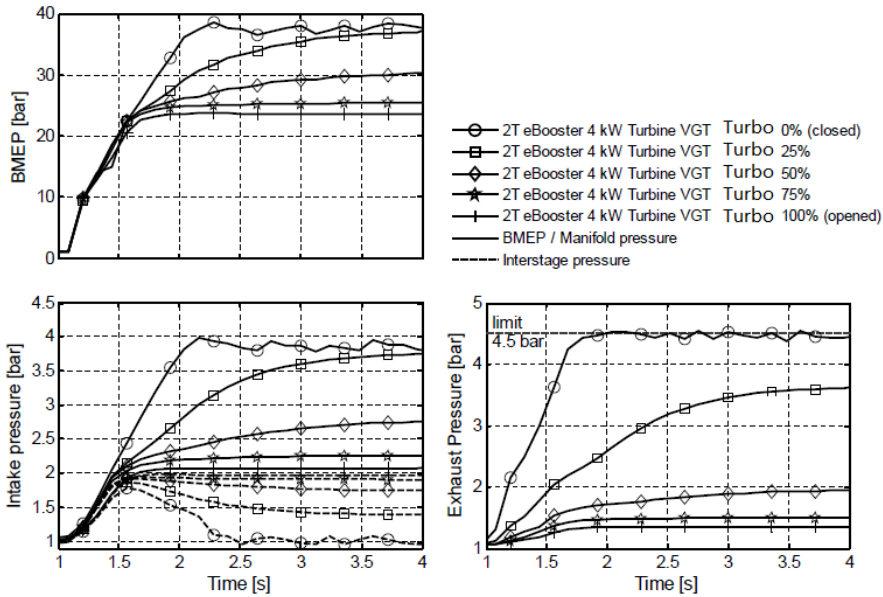


Figure 8: 2T eBooster architecture transient responses as a function of turbocharger boost abilities during cold transient test cycles at 1000rpm on the 2.3l engine.

149 in figure 8. The VGT position has been varied here to represent different turbocharger boost  
 150 abilities at low speeds. Using a relatively small matching, it has to be noticed that the main  
 151 compressor may get into surge for the closest VGT openings (see figure 9).

152 Regarding the intake pressure built-up, the transient response can be di-  
 153 vided in two different parts. First, the eBooster provides the boost correspond-  
 154 ing to the electric power in approximately 0.5 second. Then, if the turbine can produce some power under these low gas  
 155 mass flows, the turbocharger will continue to accelerate according to its efficiencies, inertia  
 156 and swallowing ca-  
 157 pacity. However, the resultant intake manifold pressure is not proportional  
 158 to the turbocharger compression ratio. In fact due to electric power limitations, the operating  
 159 conditions are moved in the eBooster compressor map along iso-power trajectories, see figure  
 160 9. On these trajectories, the compression ratio is reduced as the gas mass flow increases. The  
 turbocharger has therefore to largely offset this boost decrease to elevate the intake pressure.

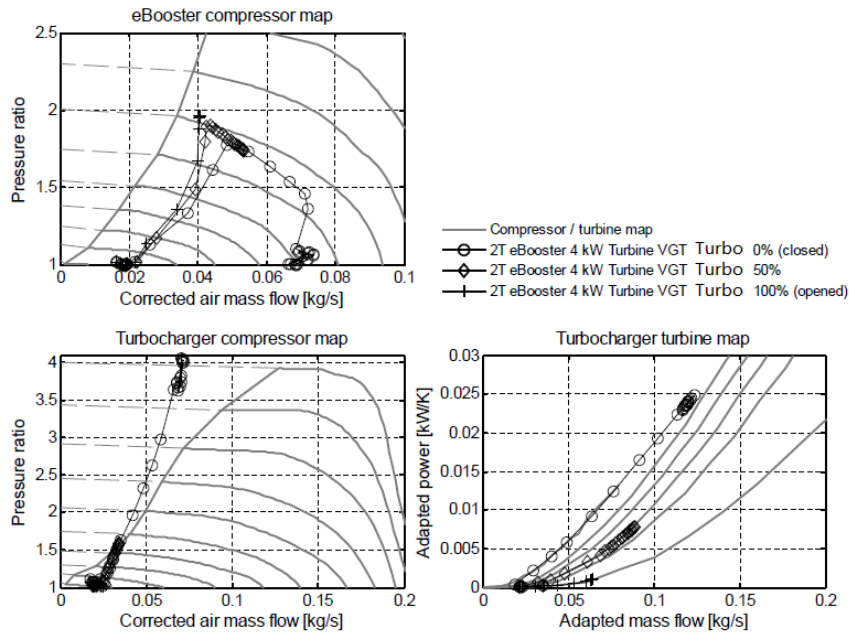


Figure 9: Transient operations plotted in the eBooster and turbocharger characteristics maps as a function of turbocharger boost abilities (cold transient test cycles at 1000rpm on the 2.3l engine). ratio

161 When 2T eBooster architecture is fitted in different engines displacement, the first part of the  
 162 time response which is mainly controlled by the eBooster characteristics is not dependant of  
 163 the engine swept volume, as shown in figure 10. Both 20 bar and 30 bar BMEP objectives  
 164 can thus be reached in approximately 0.5 second on the different downsized engines if the  
 165 eBooster and vehicle network are designed to the corresponding electric power levels. Other-  
 166 wise, the eBooster will not produce the entire boost requirements and the time response will  
 167 result slower according to the turbocharger matching and its abilities to provide the missing  
 168 compression work.

### 169 4.3 Two Stage Supercharger Architecture

170 In a 2T supercharger configuration, transient response depends on the transmission ratio, the  
 171 clutch time delay characteristics and on the turbocharger boost abilities. Without interactions

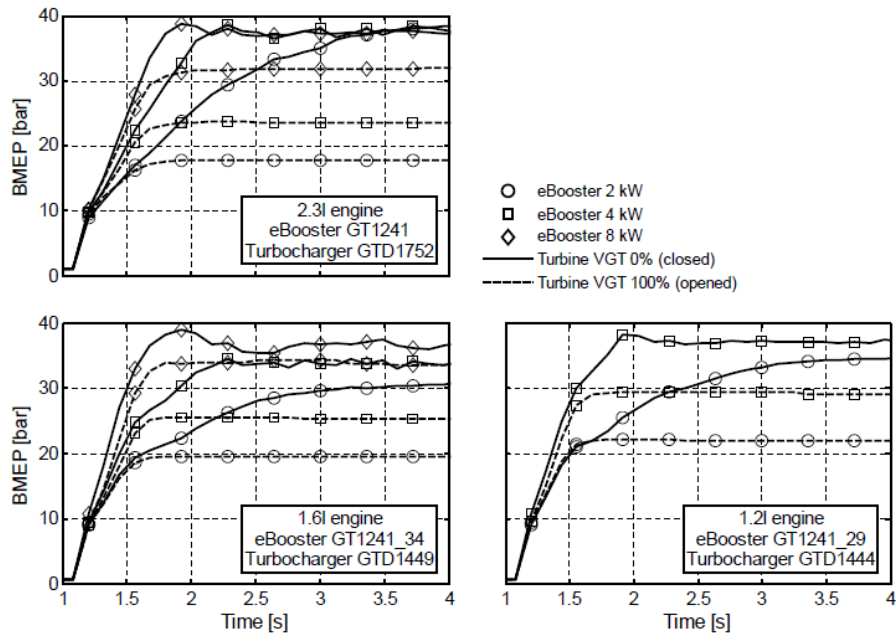


Figure 10: 2T eBooster architecture transient responses on different downsized-downspeeded engines as a function of turbocharger boost abilities and electric power levels (cold transient test cycles at 1000rpm).

172 between the turbomachines in the ex-haust side, the VGT is maintained in a closed position as  
 173 for the 2T eBooster architecture. To analyze the main characteristics of 2T supercharger sys-  
 174 tems responses, simulations have been performed on the 2.3l engine with an Eaton R250 and a  
 175 like turbocharger(GTD1752). Two different transmission ratios have been selected for the cal-  
 176 culations. The first one (rgearbox 13) corresponds to the transmission ratio which maximizes  
 177 the compression ratio avoiding over- shoots in the supercharger map (2.5 maximum compres-  
 178 sion ratio). While the second one (rgearbox 10) is relatively smaller to carry out a sensitivity  
 179 anal- ysis of the transmission ratio. In this second case, the supercharger runs at lower speeds  
 180 with a maximum compression ratio of 2 during the transient. For supercharger engagement, a  
 181 progressive activation time of 0.3 second has been retained to reproduce the behavior of typical  
 182 electromagnetic particle clutch or plate type friction clutch [146, 175]. The obtained results  
 183 are shown in figures 11-12 where VGT positions have also been varied to represent different

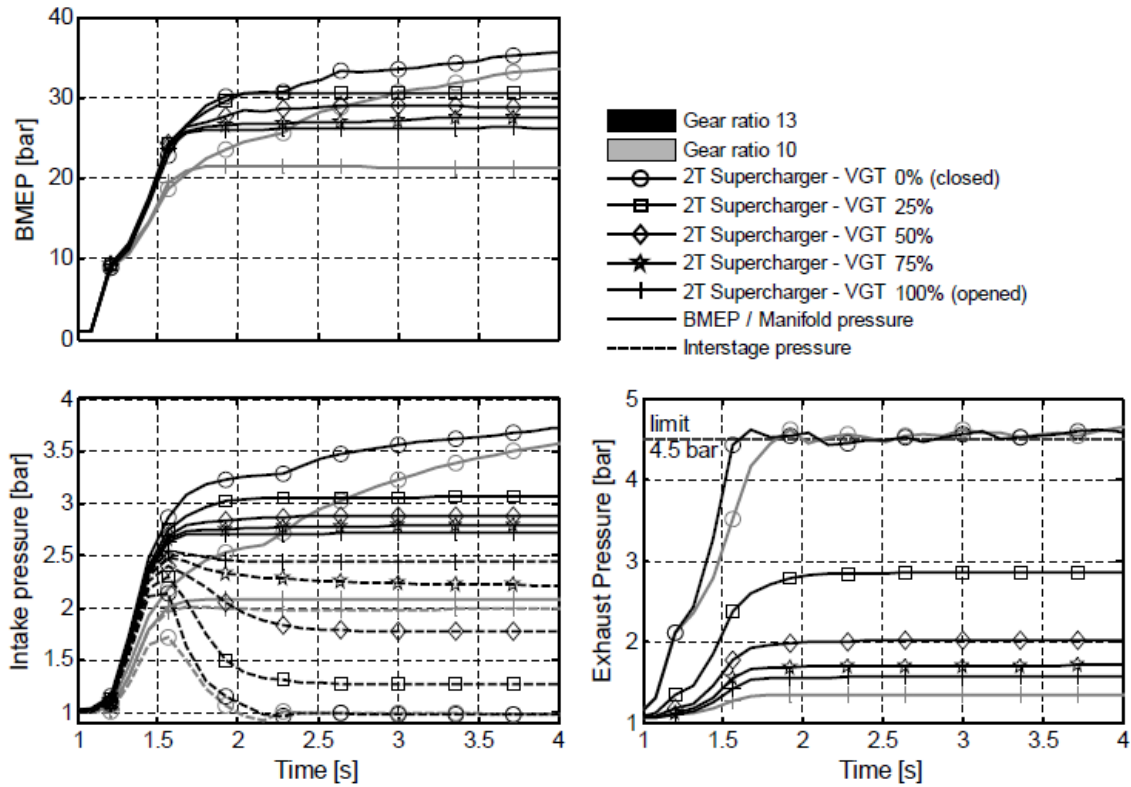


Figure 11: 2T eBooster architecture transient responses on different downsized-downspeeded engines as a function of turbocharger boost abilities and electric power levels (cold transient test cycles at 1000rpm).

184 turbocharger boost abilities.

185 In figure 11, it can be seen the supercharger provides directly at the end of its activation  
 186 time the maximum boost corresponding to the transmission ratio. The first part of the transient  
 187 is thus characterized by the clutch performance and the choice of the transmission ratio which  
 188 is crucial to reach the low-end torque objectives. In the second part, as for the 2T eBooster  
 189 configuration, the turbocharger can continue to accelerate according to its efficiencies, inertia  
 190 and swallowing capacity. However, the intake pressure increase is much more limited here  
 191 despite high reachable turbocharger compression ratios. In fact, the supercharger is a volumetric  
 192 machine which runs during this transient test cycle at constant speed ( $r_{gearboxNmot}$ ). Being

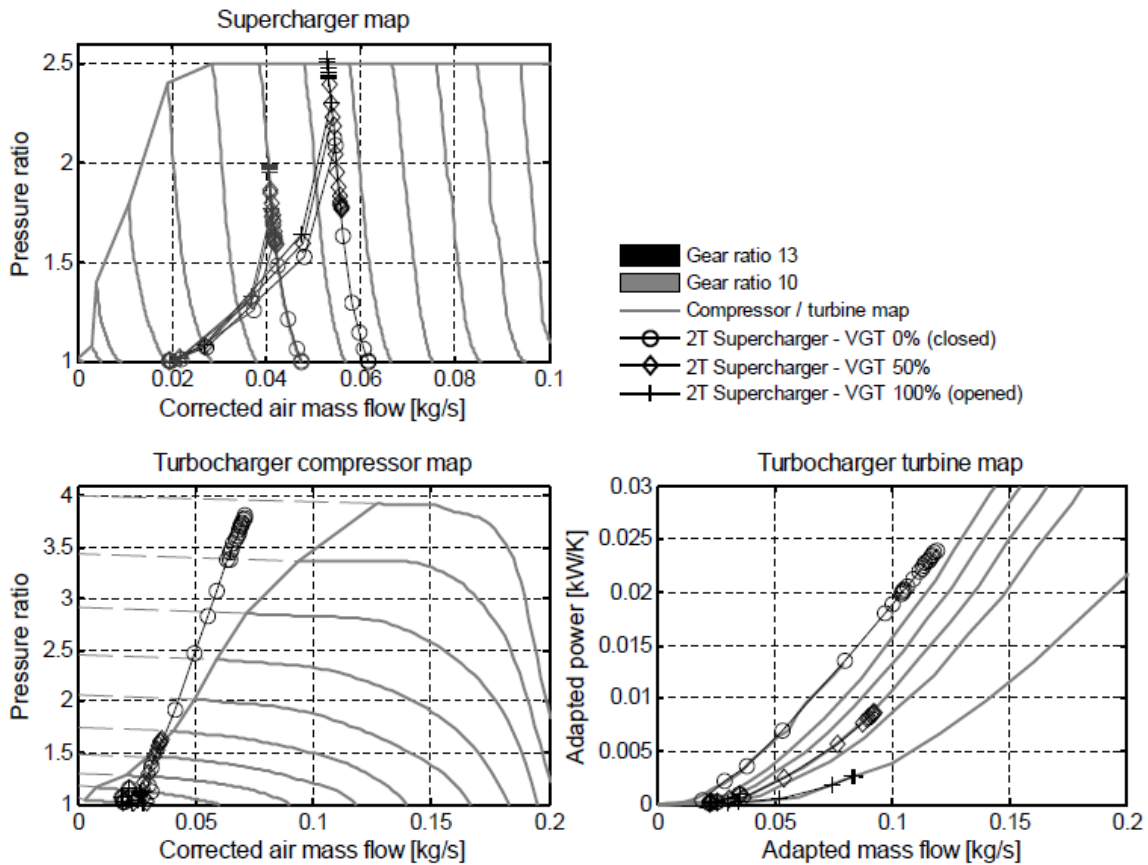


Figure 12: Transient operations plotted in the supercharger and turbocharger characteristics maps as a function of gear ratio and turbocharger boost abilities (cold transient test cycles at 1000rpm on the 2.3l engine).

193 placed upstream the turbocharger, there is no significant air density variation at its inlet. The  
 194 gas volumetric flows and the corresponding gas mass flows are thus relatively constant. Only  
 195 a slight increase can be observed in the supercharger map (figure 12) as the compression ratio  
 196 decreases due to lower internal losses.

197 So when the turbocharger accelerates and produces some boost, the gas mass flow is strongly  
 198 restricted by the supercharger volumetric capacity and the supercharger compression ratio is re-  
 199 duced creating certain equilibrium between both chargers. Until completely offsetting this boost  
 200 decrease to disengage the supercharger, the intake pressure can only suffer small variations and



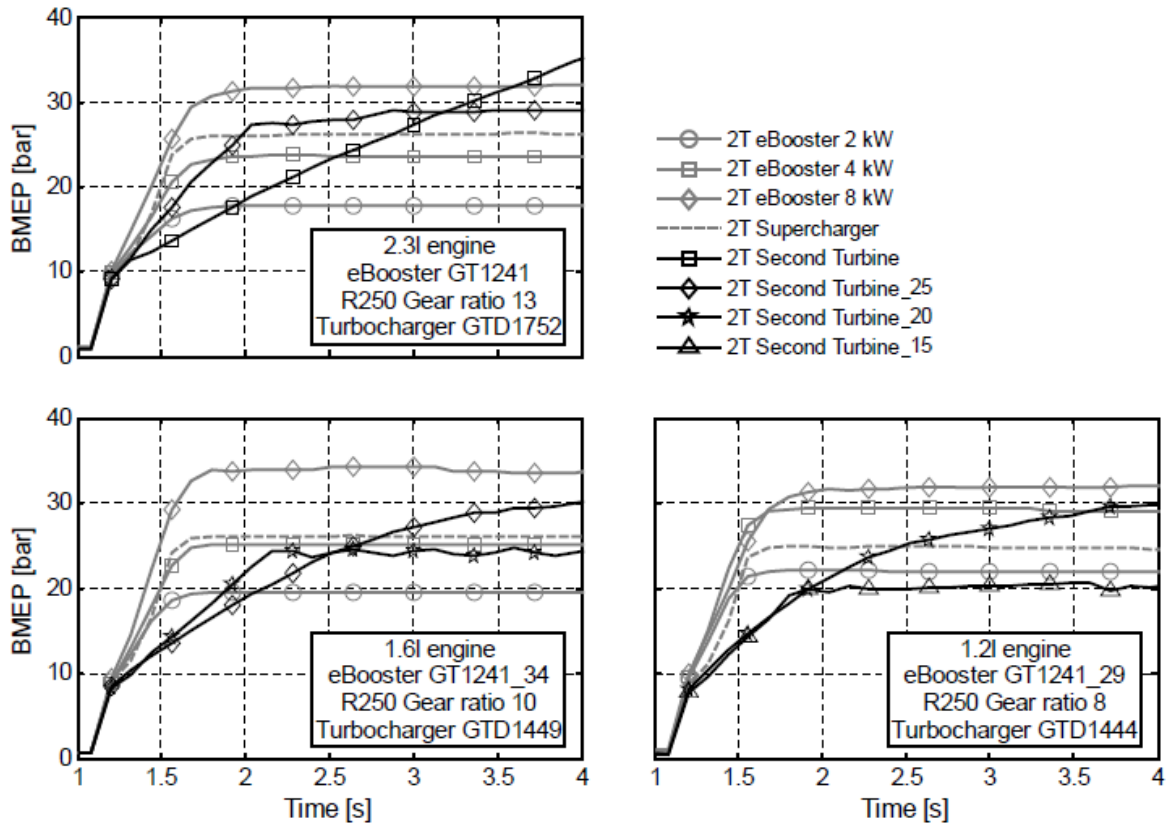


Figure 13: Synthesis of 2-Stage architecture transient performance on different downsized-downspeeded engines during cold transient test cycles at 1000rpm.

201 the BMEP increases noticed in figure 11 are the result of both slightly higher gas mass flows  
 202 and lower supercharger brake power consumptions.

203 With the same Eaton supercharger, the time responses obtained for the other engine dis-  
 204 placements are shown in figure 13. In each case, the trans- mission ratio has been optimized to  
 205 maximize the supercharger compression ratio, while the VGT has been maintained fully open  
 206 to reproduce typical matching (limited turbocharger boosting abilities at low speeds). As it can  
 207 be observed with this boosting architecture, an objective of 20 bar BMEP can be reached in  
 208 approximately 0.5 second independently of the engine swept vol- ume. Only the transmission  
 209 ratio has to be reduced to adapt the supercharger speed to the low-end torque requirement. For

210 an objective of 30 bar BMEP, as already explained, the current designs with maximum com-  
211 pression ratio of 2.5 do not allow this power level to be reached. But if new superchargers able  
212 to work under high compression ratios are developed, the same fast transient responses will be  
213 achieved.

214 In figure 13, the results obtained with the other architectures have also been plotted to an-  
215 alyze the different systems. Having almost instantaneous time responses, the transient perfor-  
216 mance of 2T supercharger and 2T eBooster configurations are obviously quite similar. However  
217 the time responses of 2T turbocharging architectures are slower and turbo-lags make perfor-  
218 mance objectives of 1 second quite challenging on the smaller engine displacements. The final  
219 architecture selection will thus depend on the future development of small high efficient tur-  
220 bochargers and, if these turbochargers are not available, the choice between the 2T supercharger  
221 and 2T eBooster systems will depend on the evolution of vehicle architecture electrification.

## 222 **4.4 Conclusion**

223 In transient operations, the turbo-lag of small turbochargers has first been characterized with  
224 sensibility studies on turbine size, shaft inertia and tur- bocharger efficiencies. Then, the other  
225 specific factors affecting transient responses such as eBooster characteristics, supercharger  
226 transmission ratio, clutch delay time, etc. . . have been analyzed putting special emphasis  
227 on con- trol strategies and main turbocharger boosting abilities at low speeds. Finally, an ar-  
228 chitecture comparison has been carried out on different downsized engines to determine the  
229 greatest transient performance that can be achieved with ad- vanced charging systems. In this  
230 chapter, most of the obtained conclusions play an integral part of the thesis contributions. So  
231 for the sake of brevity, only a summary of the performed analyses have been given here and all  
232 the corresponding conclusions have been directly reported in the following chapter specifically  
233 devoted to this purpose.

## 234 **References and Notes**

- 235 1. Carlo Beatrice, Giovanni Avolio, Nicola Del Giacomo, and Chiara Guido. Compression  
236 ratio influence on the performance of an advanced single-cylinder diesel engine operating  
237 in conventional and low temperature combustion mode. Technical report, SAE Technical  
238 Paper, 2008.
- 239 2. Alberto A Boretti and Giuseppe Cantore. Similarity rules and parametric design of race  
240 engines. Technical report, SAE Technical Paper, 2000.
- 241 3. Enrico Cacciatori, Baptiste Bonnet, Nicholas D Vaughan, Matthew Burke, David Price, and  
242 Krzysztof Wejrzanowski. Regenerative braking strategies for a parallel hybrid powertrain  
243 with torque controlled ivt. Technical report, SAE Technical Paper, 2005.
- 244 4. G Cantore and E Mattarelli. Similarity rules and parametric design of four stroke motogp  
245 engines. Technical report, SAE Technical Paper, 2004.
- 246 5. A Chasse, P Moulin, P Gautier, A Albrecht, L Fontvieille, A Guinois, and L Doléac. Double  
247 stage turbocharger control strategies development. *SAE International Journal of Engines*,  
248 1(2008-01-0988):636–646, 2008.
- 249 6. G Cipolla, A Vassallo, AE Catania, Ezio Spessa, C Stan, and L Drischmann. Combined  
250 application of cfd modeling and pressure-based combustion diagnostics for the develop-  
251 ment of a low compression ratio high-performance diesel engine. Technical report, SAE  
252 Technical Paper, 2007.
- 253 7. J Galindo, JR Serrano, C Guardiola, and C Cervelló. Surge limit definition in a specific  
254 test bench for the characterization of automotive turbochargers. *Experimental Thermal and*  
255 *Fluid Science*, 30(5):449–462, 2006.

- 256 8. José Galindo, A Tiseira, FJ Arnau, and R Lang. On-engine measurement of turbocharger  
257 surge limit. *Experimental Techniques*, 37(1):47–54, 2013.
- 258 9. Francisco Payri González and José M<sup>a</sup> Desantes Fernández. *Motores de combustión interna*  
259 *alternativos*. Editorial Universitat Politècnica de València, 2011.
- 260 10. Hermann Hiereth and Peter Prenninger. *Charging the internal combustion engine*. Springer  
261 Science & Business Media, 2007.
- 262 11. P Hoecker, JW Jaisle, and S Munz. The ebooster from borgwarner turbo systems-the key  
263 component for a new automobile charging system. *Borg Warner Turbo Systems Knowledge*  
264 *Library*, page 5, 2000.
- 265 12. N.Ausserhofer M.Weissbaeck O.Soustelle P.Ragot P. Mallet M.F.Howlett, W.Schnider and  
266 J. Rozen. 3 cylinder aggressive downsized diesel. 2010.
- 267 13. S Münz, M Schier, HP Schmalzl, and T Bertolini. ebooster design and performance of a  
268 innovative electrically driven charging system, 2008.
- 269 14. Alexandros Plianos and Richard Stobart. Modeling and control of diesel engines equipped  
270 with a two-stage turbo-system. Technical report, SAE Technical Paper, 2008.
- 271 15. José Ricardo Hector, Galindo Lucas. *Contribución a la Mejora del Margen de Bombeo en*  
272 *Compresores Centrífugos de Sobrealimentación*. PhD thesis, 2011.
- 273 16. Gino Sovran. The impact of regenerative braking on the powertrain-delivered energy re-  
274 quired for vehicle propulsion. Technical report, SAE Technical Paper, 2011.
- 275 17. Richard Van Basshuysen and Fred Schäfer. *Internal combustion engine handbook-basics,*  
276 *components, systems and perspectives*, volume 345. 2004.

- 277 18. G. Oberholz V.Simon and M. Mayer. *The Impact of Regenerative Braking on the*  
278 *Powertrain-Delivered Energy Required for Vehicle Propulsion.* Bog Warner Turbo Sys-  
279 tem Knowledge Library, 2000.
- 280 19. Neil Watson and Marian Stefan Janota. *Turbocharging: The internal combustion engine.*  
281 MacMillan, 1982.